Dependence of Melting (Liquidus) Temperature for Fiberglass-Related Compositions

Theodore M. Besmann
Oak Ridge National Laboratory
Oak Ridge, TN 37831-6063

Hong Li
PPG Industries, Inc.
Pittsburgh, PA 15230-2844

Introduction

PPG Fiber Glass group is requested DOE GMIC support in an effort to reduce fiber glass emissions while maintaining the current or reduced energy consumption of the glass fiber process. A brief overview of the emissions and energy concerns follow below.

Air emission impacts from fiber glass manufacturing are a significant motive for reformulating the glass composition in order to meet environmental regulatory requirements. Emissions from fiber glass manufacturing include pollutants generated from combustion of fuels as well as losses from the glass melting process. Nitrogen oxides (NOx) are the primary pollutants of concern from the combustion process. PPG has achieved significant NOx emission reductions over the last several years by converting most of its furnaces from air to oxygen fuel for the combustion process. Emissions from the glass melting process include particulate matter from batch raw materials and volatilized losses of boron and fluoride from the melted glass. The process pollutants are regulated by air permit requirements and state and federal air regulations that continue to become more stringent over time. Efforts to reduce pollutants include end-of-process emission control devices and/or reformulation of the glass to reduce or eliminate pollutants of concern. Pollution control devices, while effective, are costly to implement. Based on first principals, removing or reducing the air pollutants in the glass is the preferred method, and is commercially accepted based on the chemical definition for fiber glass reinforcements (ASTM D 578).

Reformulating glass to reduce or eliminate process pollutants however impacts energy consumption in the following ways. Boron and fluorine help to reduce the viscosity of the glass. Boron also reduces liquidus and provides desirable electrical properties while fluorine reduces surface tension. A reformulated glass with lower boron and fluoride removal, therefore, is expected to have significantly higher melting and forming temperatures. This higher viscosity not only increases the fossil energy required to make product but negatively impacts the electrical energy use since fibers are formed, or attenuated, through an electrically heated platinum bushing. The increased process temperatures not only require higher energy, but also are detrimental to the platinum bushings. Reducing bushing life due to accelerated bushing creep and precious metal losses for producing new fibers at higher forming temperature is expected over the standard glass formulations.

Of course, changing one part of the process, such as composition, requires changes to the other parts of the process. This includes, but is not limited to, bushing redesign to

account for higher temperatures and higher surface tensions. Finally, the glass composition changes result in a different glass surface and impact how sizing chemistry is applied and may impact final product performance.

Thus, the changes to the process can result in lost process efficiencies. Hence it is desirable to make these changes within the constraints of the process; energy costs, batch costs, maintained process efficiencies, as well as have little to no detrimental impact on electrical, mechanical, and visual properties of the glass fibers.

The focus of the current effort was to explore the effects of compositional change on melting (liquidus) temperature. The objective is to mitigate the effect of increased liquidus temperature due to changing glass composition to reduce pollutants. Thus information was obtained from equilibrium phase relations calculations, particularly looking at the influence of B_2O_3, MgO, and CaO on simplified/model fiberglass compositions.

Thermochemical Caculations

The thermochemical calculations were performed utilizing the FactSage thermochemical software package. The software allows “targeted” calculations such that the equilibrium state at the liquidus temperature for a given composition can be directly determined, avoiding the need to perform calculations across temperature space.

The thermochemical data used was that provided with FactSage. The database consists of Scientific Group Thermodata Europe (SGTE) compound values and the models for the liquid phase as provided with FactSage based on the quasichemical model. A current DOE program is developing models utilizing the associate species approach, however these were not available for the systems of interest at the time the calculations were performed.

The calculations were organized to investigate 'the effect on liquidus temperature of departures from central compositions at the eutectics in the Al_2O_3-CaO-SiO_2 and Al_2O_3-MgO-SiO_2 systems (Table I) that included additions of B_2O_3.

Table I. Eutectic Compositions.

Eutectic	**Wt.% Al_2O_3**	**Wt.% MgO**	**Wt.% CaO**	**Wt.% SiO_2**
Al_2O_3-MgO-SiO_2	18.22	21.12	-	60.66
Al_2O_3-CaO-SiO_2	12.61	-	23.53	63.85

Results

Two series of calculations were performed, each around the central eutectic compositions of either Al_2O_3-CaO-SiO_2 or Al_2O_3-MgO-SiO_2.

Al_2O_3-CaO-SiO_2 Eutectic Central Composition:

The calculations were performed assuming the added weights of MgO and B_2O_3 simply diluted the wt.% of the Al_2O_3, CaO, and SiO_2 eutectic. Figures 1 and 2 are plots of the effects of MgO and B_2O_3 alone, with the wt.% of those components shown as the actual values after addition to the eutectic composition. Also plotted is the effect of the ratios of MgO and B_2O_3 (Figs. 3 and 4). There are significant differences in the first and second crystalline phases forming as a function of composition, which may explain some of the sharp slope changes. The melting temperatures for combined MgO-B_2O_3 representative compositions in the eutectic are seen in Table II along with the first and second phases that form.

Table II. Liquidus temperatures for the Al_2O_3-CaO-SiO_2 eutectic with MgO and B_2O_3. and the first and second phases that form

T °C	MgO	B_2O_3	1st Phase	2nd Phase
1175	0	0	N/A	N/A
1162	0.971%	1.942%	tridymite	pseudowollastonite
1151	1.852%	5.556%	tridymite	pseudowollastonite
1224	4.348%	8.696%	$Mg_2B_2O_5$	tridymite

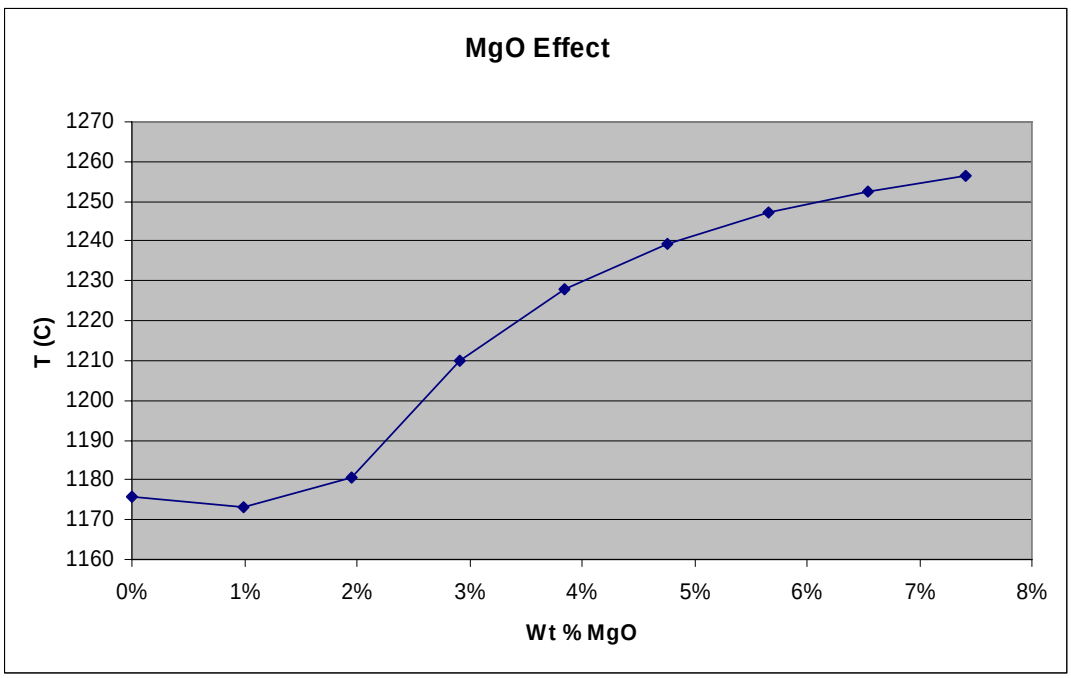

Fig. 1. Effect on liquidus temperature of weight percent addition of MgO to the eutectic composition.

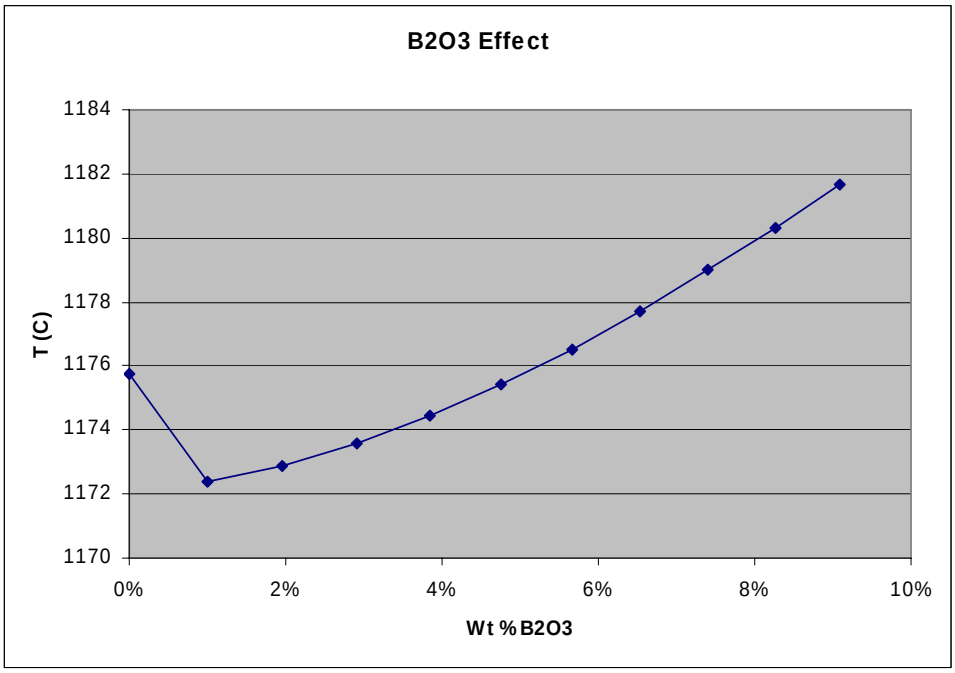

Fig. 2. Effect on liquidus temperature of weight percent addition of B_2O_3 to the eutectic composition.

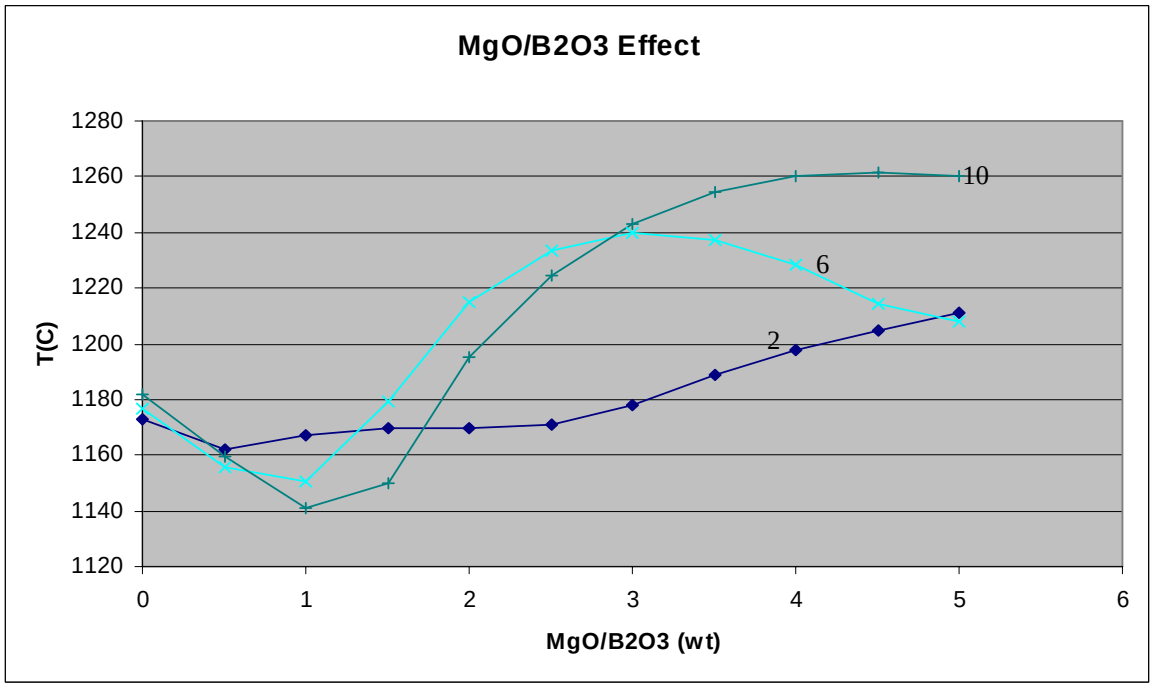

Fig. 3. Effect of MgO/B_2O_3 weight ratio on the liquidus temperature through additions to the eutectic composition. The values on the curves indicate the constant B_2O_3 added weight (to initial values of the eutectic of 100).

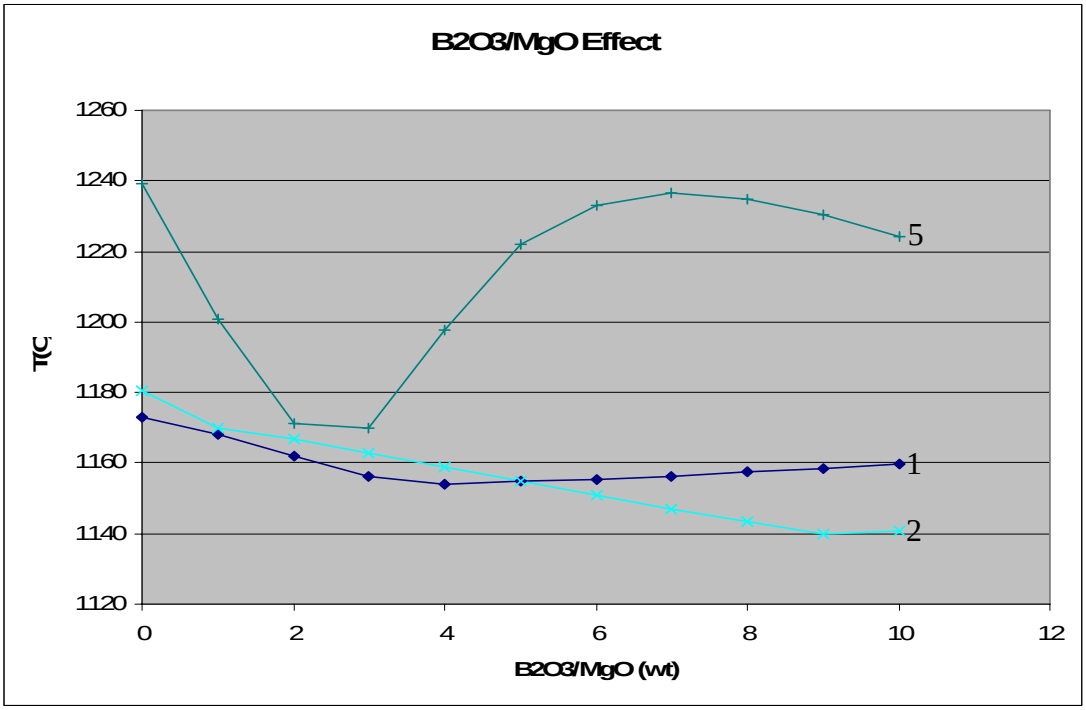

Fig. 4. Effect of B_2O_3/MgO weight ratio on the liquidus temperature through additions to the eutectic composition. The values on the curves indicate the constant MgO added weight (to initial values of the eutectic of 100).

Al_2O_3-MgO-SiO_2 Eutectic Central Composition:

The calculations were now performed assuming the added weights of CaO and B_2O_3 again simply diluted the wt.% of Al_2O_3, MgO, and SiO_2 eutectic. Figures 5 and 6 are plots of the effects of MgO and B_2O_3 alone, with the wt.% of those components shown as the actual values after addition to the eutectic composition. Figures 7 and 8 are the effect of the ratios of CaO and B_2O_3. The melting temperatures for combined CaO-B_2O_3 representative compositions in the eutectic are seen in Table III along with the first and second phases that form.

Table III. Liquidus temperatures for the Al_2O_3-MgO-SiO_2 eutectic with CaO and B_2O_3. and the first and second phases that form

T °C	CaO	B_2O_3	1st Phase	2nd Phase
1369	0	0	N/A	N/A
1377	0.971%	1.942%	tridymite	protoenstatite
1405	1.852%	5.556%	tridymite	protoenstatite
1354	4.348%	8.696%	tridymite	$Mg_3B_2O_6$

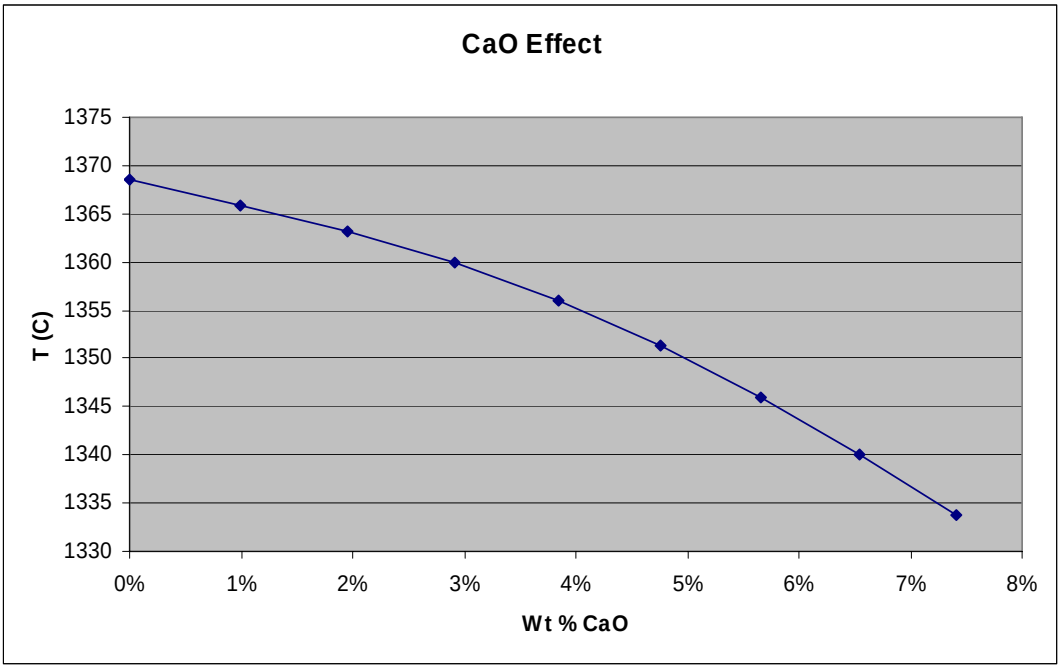

Fig. 5. Effect on liquidus temperature of weight percent addition of CaO to the eutectic composition.

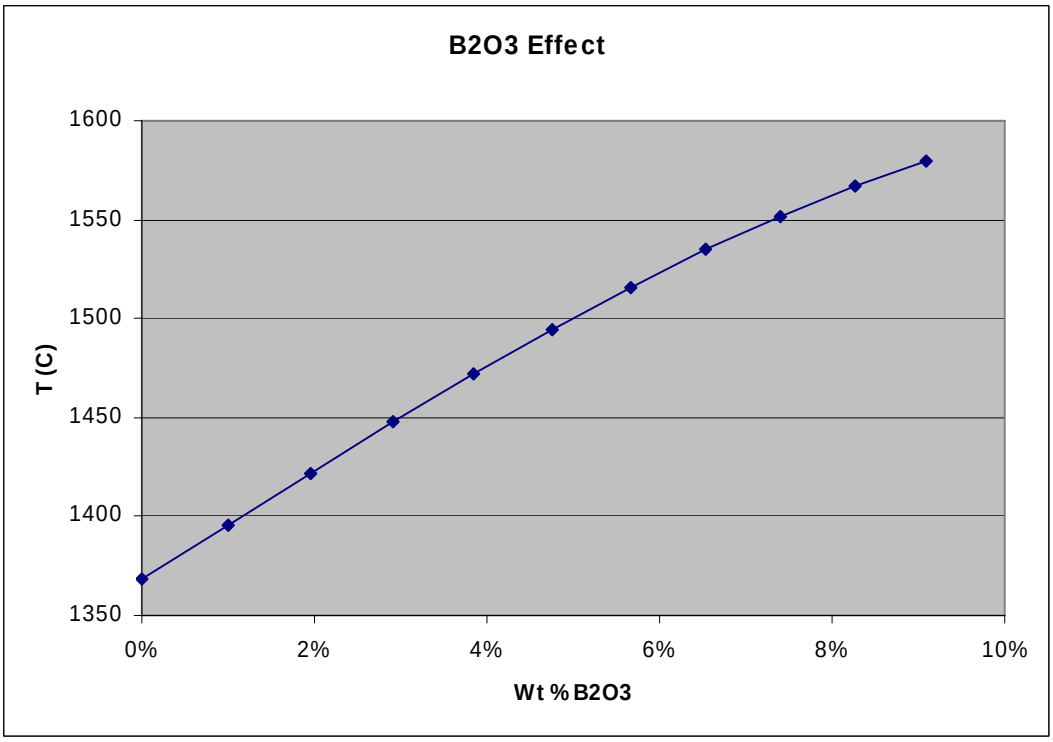

Fig. 6. Effect on liquidus temperature of weight percent addition of B_2O_3 to the eutectic composition.

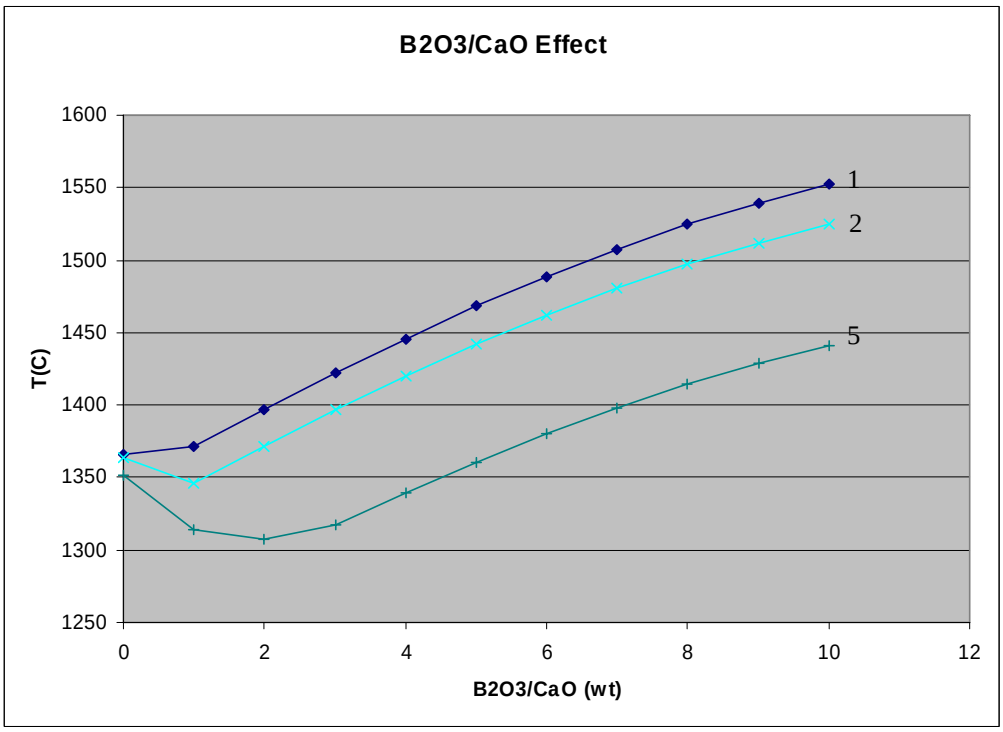

Fig. 7. Effect of CaO/ B_2O_3 weight ratio on the liquidus temperature through additions to the eutectic composition. The values on the curves indicate the constant B_2O_3 added weight (to initial values of the eutectic of 100).

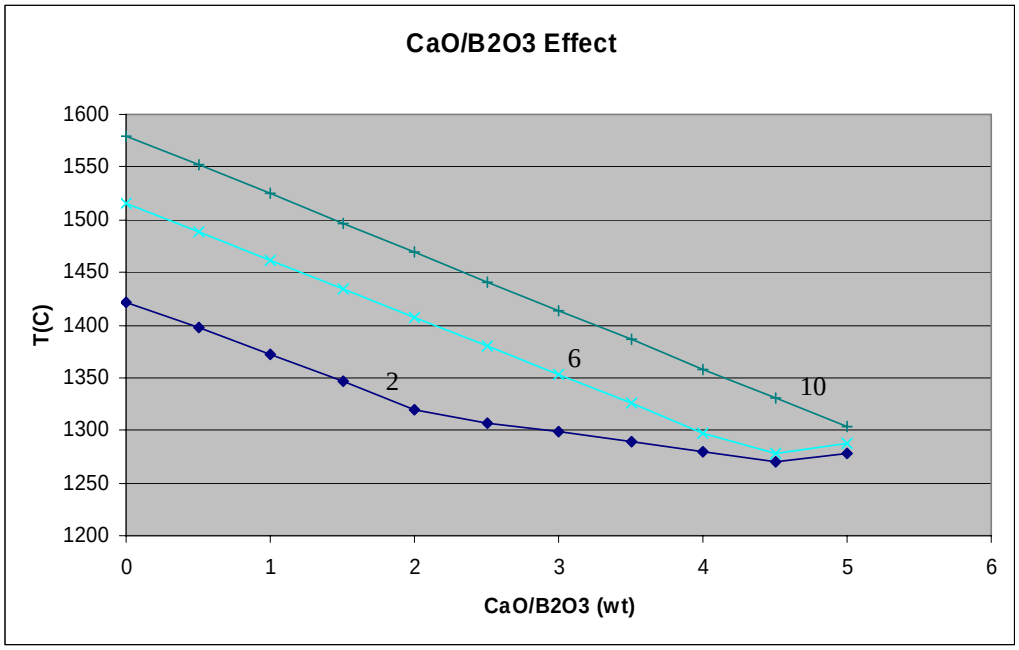

Fig. 8. Effect of B_2O_3/CaO weight ratio on the liquidus temperature through additions to the eutectic composition. The values on the curves indicate the constant CaO added weight (to initial values of the eutectic of 100).

Experimental Test of Selective Model Compositions

Selected computed liquidus temperatures (T_L^{cal}) were compared with the experimental values (T_L^{exp}) determined at PPG and the results are summarized in Table IV, along with their differences (T_L^{exp} -T_L^{cal}). Good agreements was seen in several of the systems, particularly those with little or no B_2O_3 content. The results highlight significant deficiencies in the FactSage-provided oxide liquid models for both CaO and MgO with B_2O_3 alumino-silicate systems.

Table IV. Selective Composition Tests Comparing Liquidus Temperatures from Model Calculation (T_L^{cal}) and Experiment (T_L^{exp}) (Al_2O_3 and SiO_2 equal 100 with MgO, CaO and B_2O_3 amounts incremented).

Group ID	MgO (wt%)	CaO (wt%)	B_2O_3 (wt%)	T_L^{cal} (^oC)	T_L^{exp} (^oC)	T_L^{exp} -T_L^{cal} (^oC)
e	0.00	23.53	0.00	1175.8	1254.0	-78.2
eB5	0.00	22.41	4.76	1175.4	1257.0	-81.6
eB10	0.00	21.39	9.09	1181.7	1250.0	-68.3
eM1	0.99	23.30	0.00	1173.2	1236.0	-62.8
eM3	2.91	22.85	0.00	1209.9	1210.0	**-0.1**
eM6	5.66	22.20	0.00	1247.2	1246.0	**1.2**
eM8	7.41	21.79	0.00	1256.5	1262.0	**-5.5**
e-M2b2	1.92	22.63	1.92	1166.9	1190.0	-23.1
e-M5b2	4.67	21.99	1.87	1171.1	1210.0	-38.9
e-M10b2	8.93	21.01	1.79	1211.1	1256.0	-44.9
e-M6b6	5.36	21.01	5.36	1239.5	1179.0	60.5
e-M10b6	8.62	20.29	5.17	1208.1	1212.0	**-3.9**
e-M2b10	1.79	21.01	8.93	1140.9	1210.0	-69.1
e-M4b10	3.51	20.64	8.77	1195.1	1196.0	**-0.9**
e-M5b10	4.35	20.46	8.70	1224.3	1191.0	33.3
e-M6b10	5.17	20.29	8.62	1243.0	1182.0	61.0
e-M9b10	7.56	19.77	8.40	1261.8	1173.0	88.8
e-m1B1	0.98	23.07	0.98	1168.0	1257.0	-89.0
e-m1B4	0.95	22.41	3.81	1154.1	1234.0	-79.9
e-m1B7	0.93	21.79	6.48	1156.4	1222.0	-65.6
e-m1B10	0.90	21.20	9.01	1159.6	1205.0	-45.4
e-m2B4	1.89	22.20	3.77	1158.8	1223.0	-64.2
e-m2B7	1.83	21.59	6.42	1147.0	1223.0	-76.0
e-m2B9	1.80	21.20	8.11	1140.0	1207.0	-67.0
e-m5B1	4.72	22.20	0.94	1200.6	1217.0	**-16.4**
e-m5B2	4.67	21.99	1.87	1171.1	1209.0	-37.9
e-m5B3	4.63	21.79	2.78	1170.0	1200.0	-30.0
e-m5B4	4.59	21.59	3.67	1197.5	1187.0	**10.5**
e-m5B7	4.46	21.01	6.25	1236.5	1184.0	52.5
EM2B6	1.85	21.79	5.56	1151.0	1212.0	-61.0
e	0.00	23.53	0.00	1175.8	1257.0	-81.2

Conclusions

Near the Al_2O_3-CaO-SiO_2 eutectic the addition of MgO initially reduces the liquidus temperature slightly, but it then increases substantially above 1 weight percent additions. The addition of B_2O_3 has a much weaker effect, dropping the temperature slightly through 1 weight percent addition and subsequently increasing the liquidus less than 10°C up to 9 weight percent B_2O_3. Figures 3 and 4 indicate that significant liquidus temperature reductions are possible through approximately equal 10 wt.% additions of MgO and B_2O_3.

Compositional changes from the Al_2O_3-MgO-SiO_2 eutectic show a monotonically decreasing liquidus with increasing CaO, conversely an increasing liquidus with increasing B_2O_3. As seen from Fig 8, the liquidus can be reduced to a minimum of approximately 1275°C through significant additions of CaO with minor amounts of B_2O_3.

Comparison with experimental results showed substantial deviations from computed liquidus values. This highlights the need for better models in these systems than those currently available through the FactSage databases. Work is ongoing in an Industrial Materials of the Future project to address some of these needs. PPG notes that significant modeling improvements for both CaO and MgO alumino-silicate will provide invaluable assistance to the fiber glass industry in predicting the impact of composition change on fiber glass processability